Uehara et al., https://doi.org/10.1085/jgp.201611624

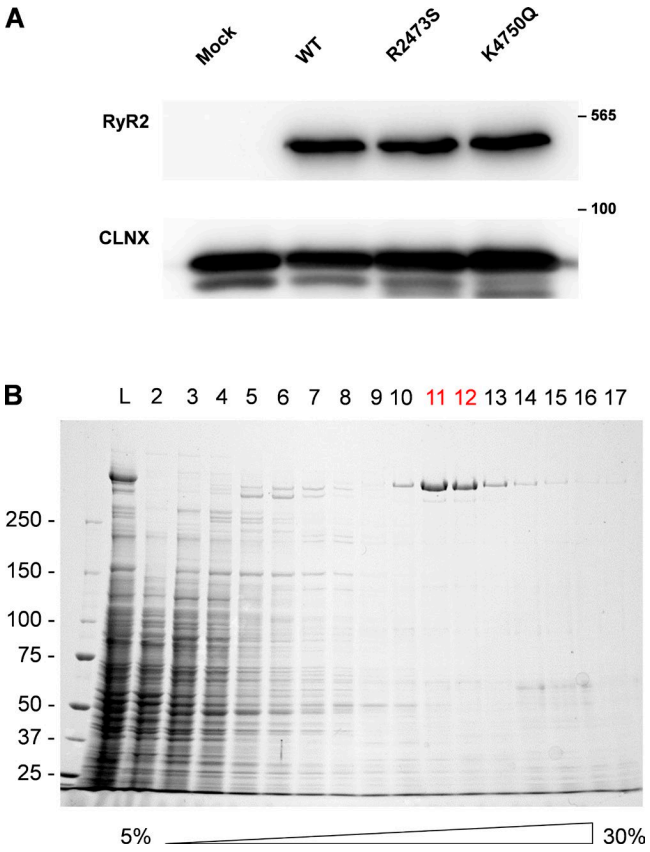


Figure S1. **Heterologous expression and isolation of recombinant RyR2 proteins.** (A) Western blotting of mouse RyR2 in the lysates from HEK293 expressing recombinant WT, R2473S, or K4750Q proteins. Calnexin (CLNX) was used as a control housekeeping protein. (B) Partial purification of the recombinant RyR2 from CHAPS-solubilized preparation by the sucrose gradient centrifugation. Lanes 11 and 12 contain the dark band corresponding a high molecular mass of RyR2 molecules. Numbers next to the blots are sizes of molecular weight standards ($M_r \times 10^{-3}$).

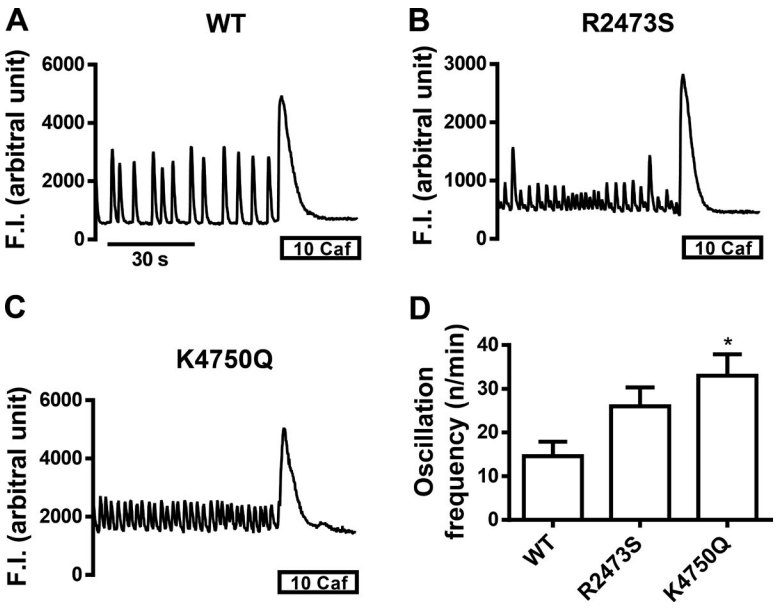


Figure S2. **G-GECO1.1 $Ca^{2+}$ signals in nonbeating cardiac HL-1 cells expressing WT and mutant RyR2s.** (A-C) $Ca^{2+}$ signals were recorded in normal Krebs solution for 60 s and then in the presence of 10 mM caffeine for 30 s. (D) $Ca^{2+}$ oscillation frequencies in normal Krebs solutions. *n* = 7, 8, and 6 for WT, R2473S, and K4750Q, respectively. *, P < 0.05 versus WT. Values shown are mean ± SEM.

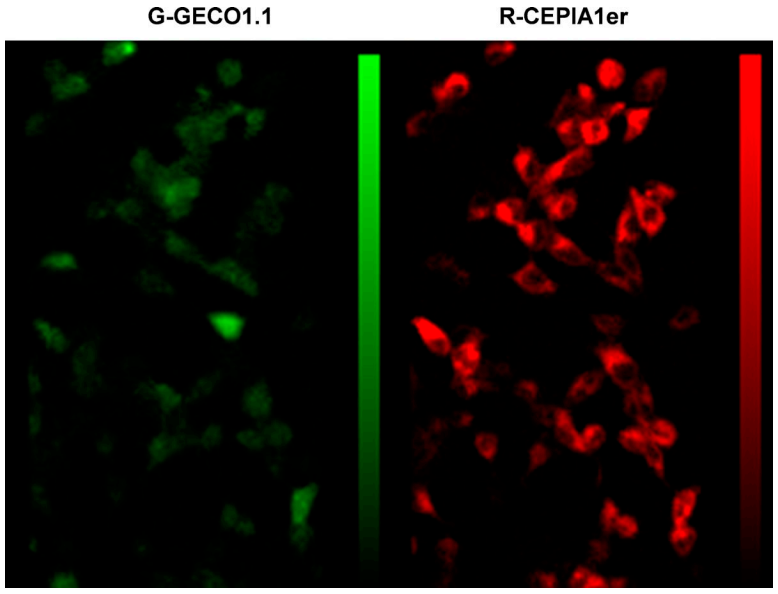


Figure S3. **Confocal $Ca^{2+}$ imaging on RyR2-expressing HEK293 cells.** Genetically encoded $Ca^{2+}$ sensors G-GECO1.1 and R-CEPIA1er were used to simultaneously examine $Ca^{2+}$ dynamics in the cytoplasm and ER lumen of cells, respectively. Spontaneous $Ca^{2+}$ oscillations were visible as alternative blinking signals in the left and right picture of Video 4.

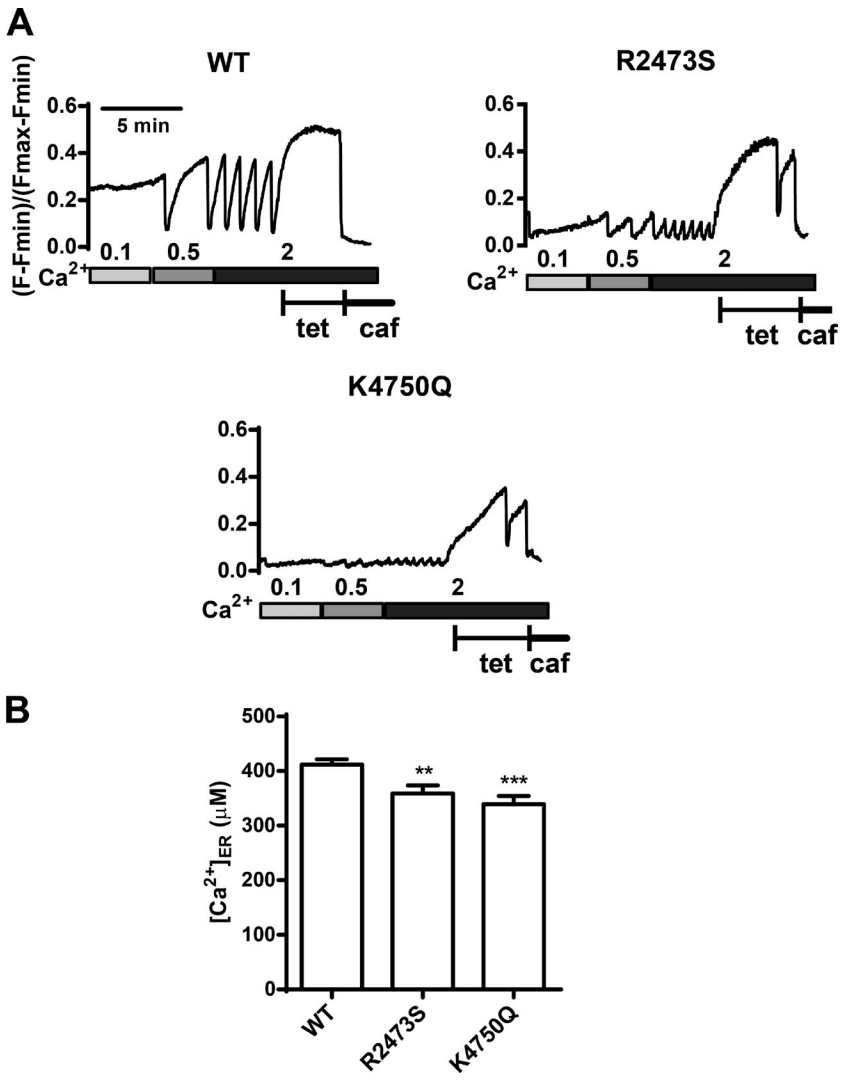


Figure S4. **Effects of tetracaine on ER $Ca^{2+}$ signals obtained with R-CEPIA1er in HEK293 cells expressing WT or mutant RyR2s.** (A) Representative ER $Ca^{2+}$ signals obtained in increasing concentrations of $[Ca^{2+}]_o$ and then in the presence of 1 mM tetracaine. (B) Mean $[Ca^{2+}]_{lum}$ in the presence of 1 mM tetracaine and 2 mM $[Ca^{2+}]_o$. *n* = 145, 91, and 70 for WT, R2473S, and K4750Q, respectively. **, P < 0.01 versus WT. ***, P < 0.001 versus WT. Values shown are mean ± SEM. Note that $[Ca^{2+}]_{lum}$ in R2473S and K4750Q cells was slightly lower than that of WT cells because occasional oscillations occurred even in the presence of tetracaine.

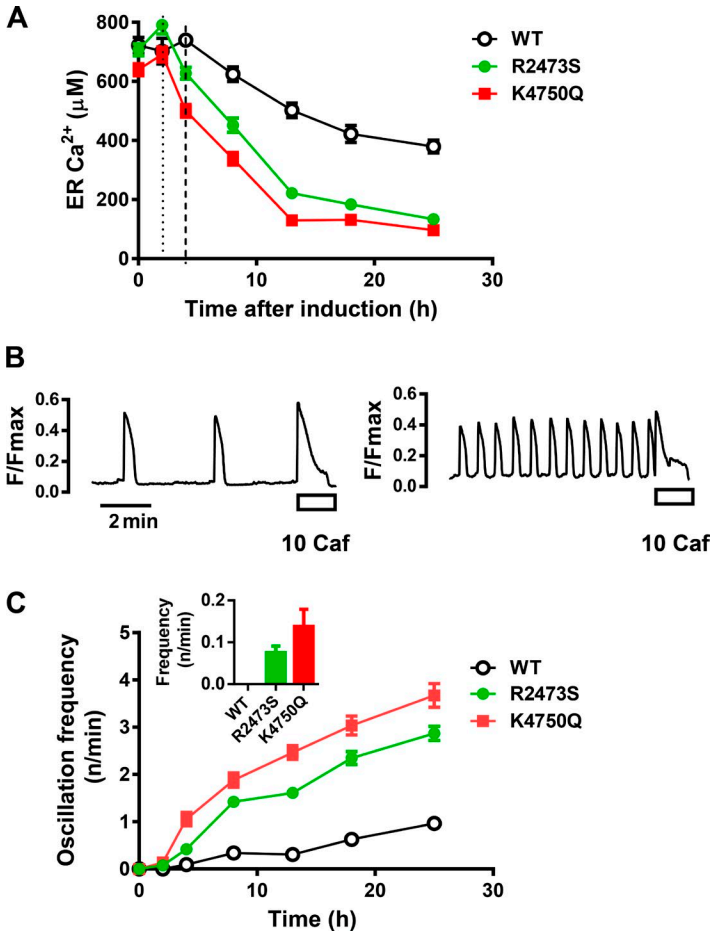


Figure S5. **Effects of RyR2 expression level on $Ca^{2+}$ homeostasis in HEK293 cells.** (A) Time course of ER $Ca^{2+}$ level was determined using R-CEPIA1er. Note that ER $Ca^{2+}$ level in K4750Q cells was similar to that of WT cells at 2 h after induction (dotted line), and slightly reduced at 4 h after induction (dashed line). (B) Representative $[Ca^{2+}]_{cyt}$ signals (fluo-4) in WT (left) and K4750Q (right) cells 4 h after induction. (C) Time course of changes in oscillation frequency of WT and R2473S- and K4750Q-expressing cells after induction. (inset) Oscillation frequency of WT and mutant RyR2 expressing cells at 2 h after induction. Values shown are mean ± SEM.

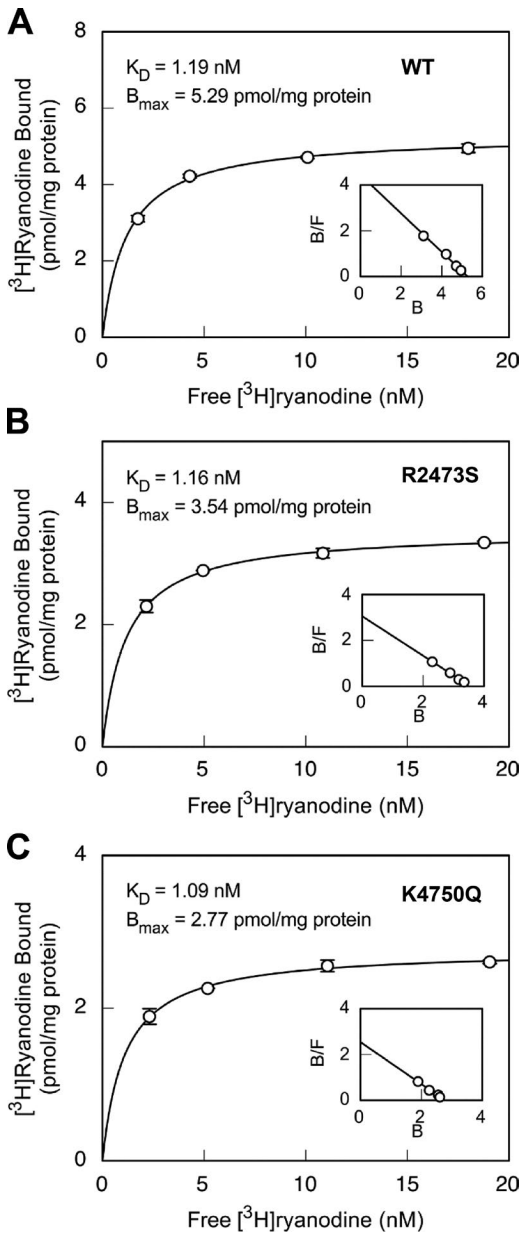


Figure S6. **Dose-dependent [$^3$H]ryanodine binding to WT and mutant RyR2 channels.** (A–C) [$^3$H]Ryanodine binding of WT (A), R2473S (B), and K4750Q (C) RyR2 channels was carried out as in Materials and methods with 3–20 nM [$^3$H]ryanodine. Linear Scatchard plots for the binding (insets) indicate that WT and mutant channels had a single class of binding sites. Means of triplicate determinations were plotted. Values shown are mean ± SEM.

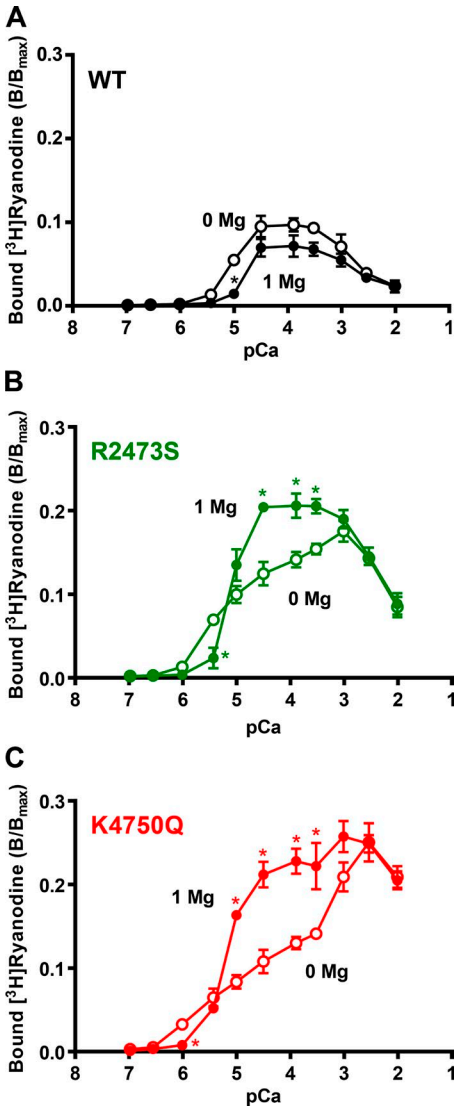


Figure S7. **$Mg^{2+}$ action on $Ca^{2+}$-dependent [$^3$H]ryanodine binding.** (A–C) WT (A), R2473S (B), and K4750Q (C) results are shown. Data points denoted by open and filled symbols were obtained in the absence and presence of 1 mM $Mg^{2+}$, respectively. Note that $Mg^{2+}$ modification pattern in the binding levels is clearly different between the three types of RyR2. Activatory action of $Mg^{2+}$ in the binding level is detected only in mutants. Means of triplicate determinations were plotted. *, $P < 0.05$ versus WT. Values shown are mean ± SEM.

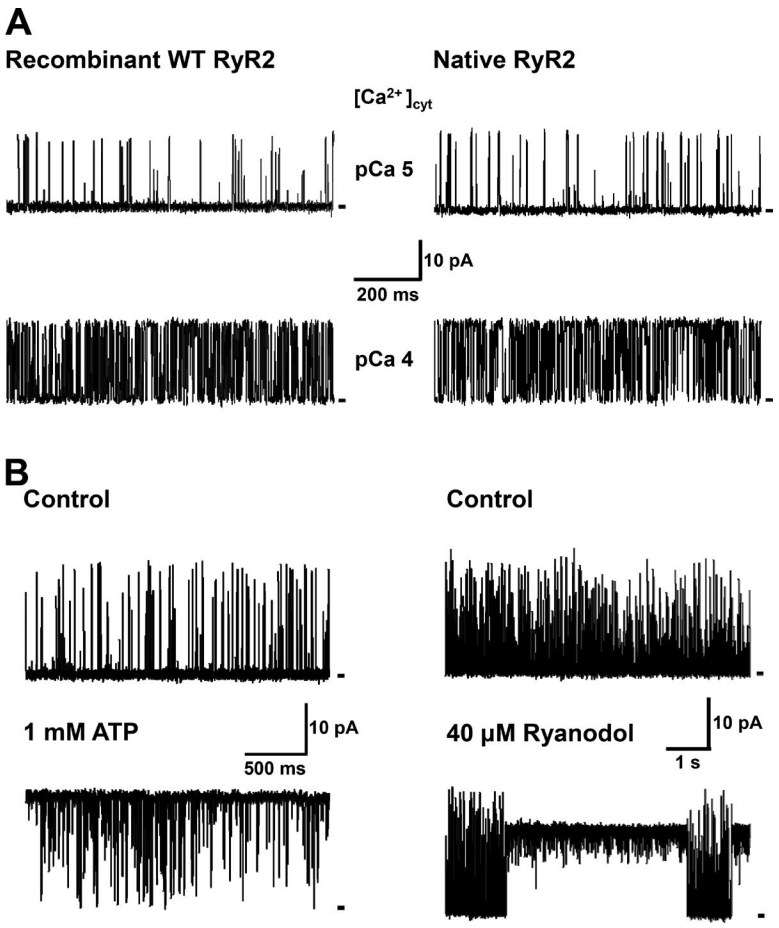


Figure S8. **Sensitivities of our single-channel currents to various RyR2 ligands.** (A) Activation of recombinant (left) and native (right) single channels upon an increase in $[Ca^{2+}]_{cyt}$ from pCa 5 (top) to 4 (bottom). (B) Activation of recombinant single channels by endogenous (left, ATP) and exogenous (right, ryanodol) ligands. Openings are upward.

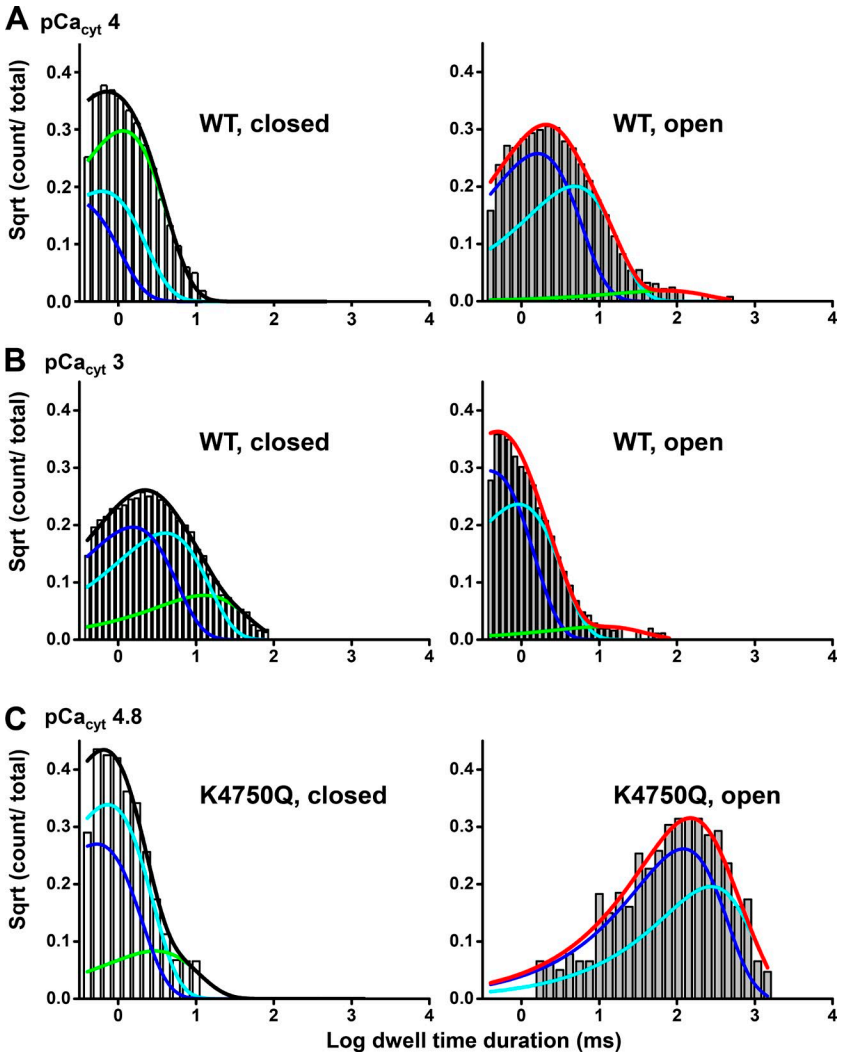


Figure S9. **Open (left) and closed (right) time histograms with exponential fittings to construct state models and simulated currents.** The histograms were obtained from single-channel currents activated by cytosolic $Ca^{2+}$ as follows. (A) WT at pCa$_{cyt}$ 4. (B) WT at pCa$_{cyt}$ 3. (C) K4750Q at pCa$_{cyt}$ 4.8. *n* = 6 for WT and mutant channels.

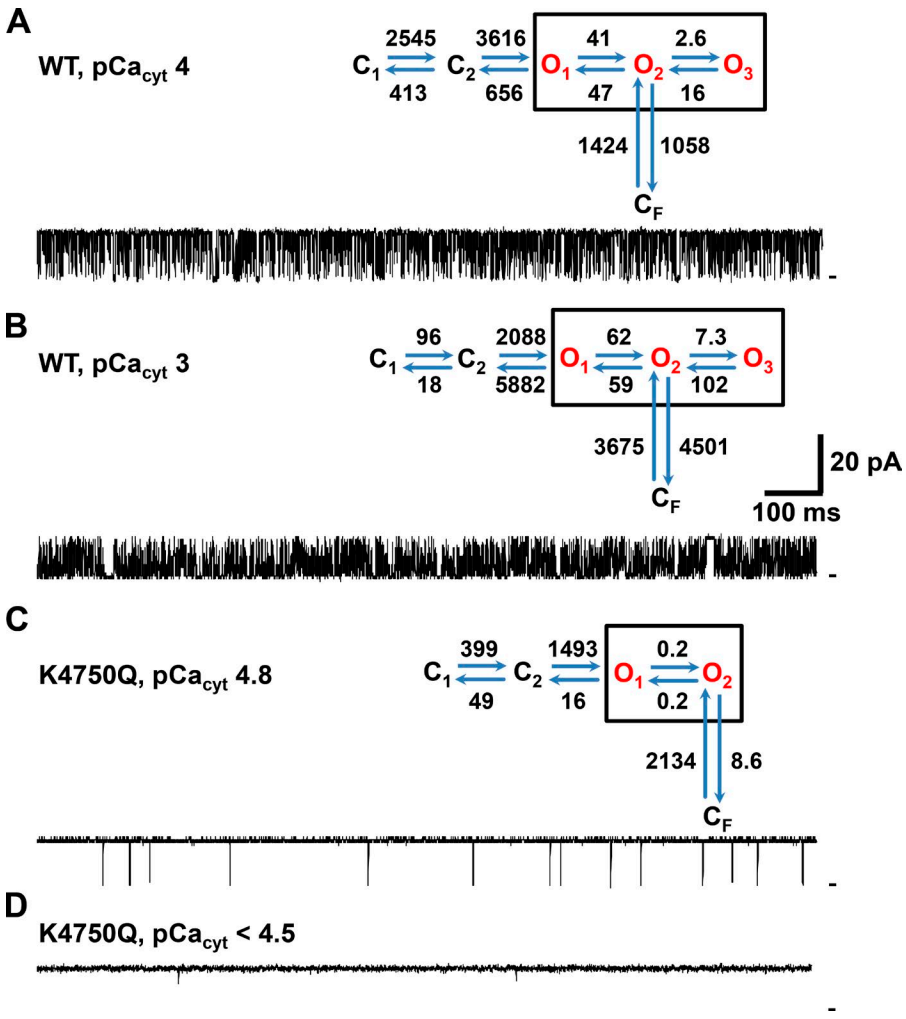


Figure S10. **State models and simulated currents focusing on $[Ca^{2+}]_{cyt}$-dependent inactivation.** (A) WT at $pCa_{cyt}$ 4: maximum likelihood value (LL) = 97,353, events = 17,594. (B) WT exhibiting the clear inactivation obtained at $pCa_{cyt}$ 3: LL = 180,776, events = 32,289. (C) Opening currents of K4750Q with brief but fully resolved closures obtained at $pCa_{cyt}$ 4.8: LL= 1,672, Events = 465. (D) Almost fully open currents lacking the inactivation of K4750Q activated by $pCa_{cyt}$ < 4.5. *n* = 6 for WT and mutant channels.

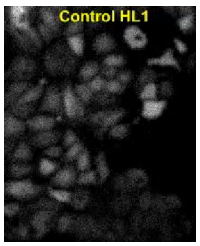


Video 1. **Cytoplasmic $Ca^{2+}$ signals in control HL-1 cells expressing no recombinant RyR2.** This video was acquired at 20 frames/s and is shown at 30 frames/s (1.6× speed).

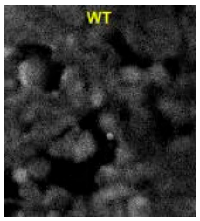


Video 2. **Cytoplasmic $Ca^{2+}$ signals in HL-1 cells expressing RyR2-WT.** This video was acquired at 20 frames/s and is shown at 30 frames/s (1.6× speed).

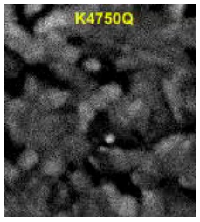


Video 3. **Cytoplasmic $Ca^{2+}$ signals in HL-1 cells expressing RyR2-K4750Q.** This video was acquired at 20 frames/s and is shown at 30 frames/s (1.6× speed).

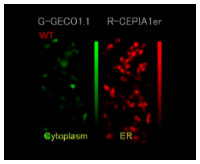


Video 4. **Cytoplasmic and ER-luminal $Ca^{2+}$ signals in HEK293 cells expressing RyR2-WT.** This video was acquired at 1.4 frames/s and is shown at 20 frames/s (14× speed).

Table S1. **List of forward and reverse primers used for construction of full-length RyR2**

| Name (base pairs) | Forward primer | Reverse primer |
|---|---|---|
| F1 (1–2,351) | 5′-GG**ACGCGT**GCCACCATGGCTGATGCGGGCGAAGGC-3′ | 5′-CC**GGTACC**ATCGATATTGAAGTTCTCAAA-3′ |
| F2 (2,351–4,404) | 5′-GG**ACGCGT**AATTATCGATGGCCTGTTCTTTCCA-3′ | 5′-CC**GATATC**CTAGGGTGACCGTCACTGTG-3′ |
| F3 (4,404–8,861) | 5′-GG**ACGCGT**AATTCCTAGGAGATGAAAAAGGAAA-3′ | 5′-CC**GCGGCCGC**GTACGGGAAGTGTTCTCCTT-3′ |
| F4 (8,861–10,185) | 5′-GG**ACGCGT**AATTCGTACGAGCAAGAAATCAAGT-3′ | 5′-CC**GGTACC**TTCGAAATAGCTCCTCTGCTT-3′ |
| F5 (10,185–14,901) | 5′-GG**ACGCGT**AAAATTCGAATGGTGGCTGAAGTCT-3′ | 5′-CC**GCGGCCGC**TAATTTAACTGGTCTTCATA-3′ |

Bold indicates additional restriction enzyme sites used for cDNA cloning for full-length *RyR2*.

Table S2. **Time constants and relative areas for exponential fits of closed and open time distributions**

| | Closed | | Open | |
|---|---|---|---|---|
| | τ | Area | τ | Area |
| | *ms* | % | *ms* | % |
| $pCa_{cyt}$ 5 | 2.57 | 6 | 0.82 | 76 |
| WT | 29.52 | 90 | 1.31 | 24 |
| Fig. 8 A | 131.77 | 4 | | |
| $pCa_{cyt}$ 5 | 1.12 | 34 | 12.10 | 45 |
| K4750Q | 2.53 | 49 | 20.94 | 55 |
| Fig. 8 A | 2.73 | 17 | | |
| $pCa_{lum}$ 4 | 2.46 | 49 | 0.30 | 25 |
| WT | 20.62 | 37 | 1.01 | 72 |
| Fig. 10 A | 194.81 | 13 | 6.58 | 3 |
| $pCa_{lum}$ 4 | 1.01 | 4 | 5.59 | 33 |
| K4750Q | 61.70 | 44 | 34.79 | 64 |
| Fig. 10 A | 268.23 | 52 | 247.68 | 3 |
| $pCa_{cyt}$ 4 | 0.25 | 8 | 1.45 | 58 |
| WT | 0.55 | 22 | 4.25 | 41 |
| Fig. S9 A | 1.02 | 70 | 61.54 | 1 |
| $pCa_{cyt}$ 3 | 1.41 | 44 | 0.36 | 46 |
| WT | 3.69 | 47 | 0.83 | 53 |
| Fig. S9 B | 11.65 | 9 | 9.91 | 1 |
| $pCa_{cyt}$ 4.8 | 0.47 | 32 | 106.14 | 64 |
| K4750Q | 0.64 | 62 | 238.54 | 36 |
| Fig. S9 C | 2.62 | 6 | | |

Listed values were obtained from the RyR2 single-channel currents at various cytoplasmic or luminal pCa in WT and K4750Q. Analogue filter, 2KHz; dead time, 0.179 ms.